The MD Simulation of Cocrystal of CL-20 with linear nitroamine materials

S. T. Wang[1]* Y. P. Hao[1] S. H. Ba[1] D. Wang[2]

1. Department of Equipment engineering, Shenyang ligong University, 6#street, Nanping Middle Road, Hunnan District, Shenyang, Liaoning Province,110159, China
2. Beijing North Vehicle Group Corporation, Beijing, China

Abstract: The existing cocrystal preparation of CL-20 is difficult to form large-scale production. And new ligands and processes are needed to change the current situation. Molecular dynamics simulation was performed on CL-20/DNDA7(3.5-dinitro-3.5-diazaheptane) and CL-20/HMX cells. Radial function analysis, Hirshfeld surface comparison analysis, and growth simulation analysis were performed on the simulation results. The results show that: Decreasing the temperature is beneficial to increase the strength of the hydrogen bond of CL-20/DNDA7 cocrystal, especially at 203K; The maximum initiation N-N bond length is smaller than that of CL-20 crystal and CL-20/HMX cocrystal; The hydrogen bond interaction of CL-20/HMX cocrystal is lower than that of CL-20/DNDA5 and CL-20/DNDA7 cocrystal. Decreasing the temperature is beneficial to cocrystal formation. The sensitivity of CL-20/DNDA7 is lower than that of CL-20 and CL-20/HMX cocrystal. CL-20 is more likely to form hydrogen bonds with linear nitroamine explosives than CL-20/HMX.

Keywords: cocrystal; Molecular dynamics simulation; hydrogen bond interaction; sensitivity

1. Introduction

2,4,6,8,10,12-hexanitro- 2,4,6,8,10,12-hexaazaisowurtzitane, commonly known as CL-20, is one of the most energetic dynamites in current energetic materials. However, its high mechanical sensitivity limits its use. In order to reduce the sensitivity of CL-20, a series of modification measures have been carried out. For example, CL-20 was used and blended with TNT to prepare the explosive mixture. However, the disadvantage is that CL-20 will change from ε-crystalline to β-crystalline when heated, which not only increases the sensitivity but also decreases the density of CL-20. [1] It is an excellent improvement method to modify CL-20 by using the advantages of cocrystal to not only retain the high energy density characteristics of CL-20 but also reduce its mechanical sensitivity. [2] Most scholars mainly focus on the experimental and simulation study of the cocrystal formation of CL-20 with cyclic explosives, such as with TNT, 1,3, 5-tri-amino-2,4, 6-trinitrobenzene (TATB), 4,10-dinitro-2,6,8,12-tetraoxa-4,10-diazatetracyclododecane (TEX), dinitrotoluene (DNT), Cyclotetramethylene

tetranitramine (HMX), Cyclotrimethylenetrinitramine (RDX), dinitrophenol (DNP), etc. [3-10] When these substances form cocrystals with energetic materials, most of them are prepared by slow solvent volatilization, [11-17] but it is time-consuming. It is difficult to form cocrystals when prepared by fast solvent evaporation, solvent/non-solvent method, [18-20] and mechanical mixing. [21-22] It is difficult to form a large-scale production, which limits the use of CL-20.

Linear nitramine energetic materials have a straight chain structure, which has its unique advantages over cyclic energetic materials. Firstly, hydrogen bonding is an important driving force for cocrystal formation. [23-27] The molecular bending and folding of linear nitramine energetic materials are greater than that of cyclic structures. We can make full use of the hydrogen atoms and their nitro group to form more hydrogen bonds with CL-20. This is also the reason why the formation of pharmaceutical cocrystals is easier than that of energetic materials. Secondly, the nitro group on linear nitramine energetic materials has a higher power supply and forms larger hydrogen bonding energy. [28]Finally, small molecule linear nitramine energetic materials have smaller steric hindrance and cocrystal cells with greater stability. Therefore, the development of CL-20 and linear nitroamine explosive cocrystals is of great significance.

This paper, selected a linear nitramine energetic material, 3.5-dinitro-3.5-diazaheptane (DNDA7) as a CL-20 cocrystal ligand. The cell configuration was established in a molar ratio of 2:1, and molecular dynamics simulation of the cell configuration at different temperatures was conducted to analyze the influencing factors of cocrystal formation. A large number of scholars have studied cyclic ligands such as CL-20/HMX cocrystal. [29-35] Therefore, compared with the simulation results of CL-20/HMX cocrystal under the same conditions, the advantages and disadvantages of the two types of CL-20 cocrystal were explored, the driving force of cocrystal formation was revealed, and the feasibility and advantages of linear ligands and CL-20 cocrystal were demonstrated, which provides a new idea for the study of the cocrystal of CL-20 and linear energetic materials.

2. Calculation method

Step 1: CL-20/DNDA7, CL-20/HMX supercell construction.

CL-20/DNDA7 cell prediction was obtained using the method of my previous research. [28] The 2*2*2 supercell is shown in Figure 1(b). The CL-20/DNDA5 cocrystal supercell is shown in Figure 1(a). According to the crystallographic database (CCDC-1919565), the CL-20/HMX cocrystal model with a molar ratio of 2:1 was established and its 2*2*2 supercell was constructed as shown in Fig. 1(c). The yellow part is CL-20 and the blue part is CL-20 cocrystal ligand.

Step 2: Supercell molecular dynamics simulation

Molecular dynamics simulation was performed on the CL-20/DNDA7 supercell. Calculations setting of MS: The forcite module was selected to use. The computational task is Dynamics. Accuracy is Ultra-fine. The force field is selected as the COMPASS force field. The task is under the domain. The Andersen temperature control and Parrinello pressure control methods are chosen. The initial velocity of the atomic motion is determined randomly according to the Maxwell-Boltzmann distribution, the integration time step is set to 1.0 fs, and the total number of simulation steps is 200,000. For the convenience of the later experiments, the temperatures were set as 203 K, 223 K, 253 K, 273 K, 303 K, and 323 K according to the temperature conditions achievable in the laboratory.

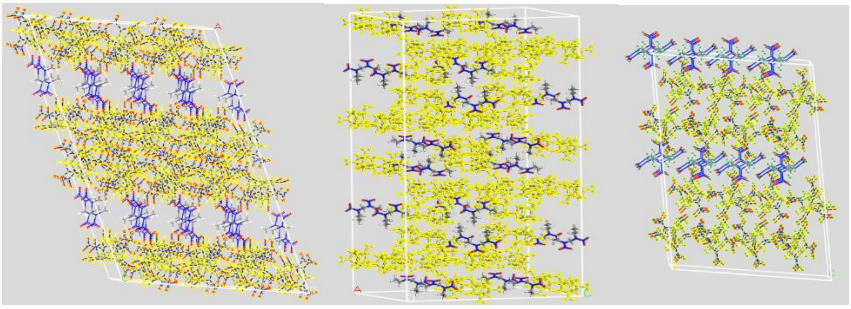

(a) (**b**) (**c**)

Figure 1. CL-20/DNDA5 (a), CL-20/DNDA7 (b) supercell, CL-20/HMX (c) supercell

3. Results and Discussion

3.1. Molecular dynamics simulation results

Variation of total energy and density of CL-20/DNDA5, CL-20/DNDA7 cocrystal at different temperatures., as shown in Table 1 and Table 2. The cocrystal energy change curve with temperature is shown in Figure 2.

Table 1. Total energy and density at different temperatures of CL-20/DNDA7 cocrystal

T(K)	203	223	253	273	303	323
Total energy (kcal·mol-1)	-20734.4	-20342.1	-19744.9	-19460.3	-18829.5	-18454.2
Max-Min (kcal·mol-1)			2280.2			
Density (g·cm-3)	1.818	1.806	1.794	1.784	1.778	1.755
Van der Waals force energy (kcal·mol-1)	-577.0	-549.4	-513.1	-429.3	-489.2	-439.6

Table 2. Total energy and density at different temperatures of CL-20/DNDA7 cocrystal

T(K)	203	223	253	273	303	323
Total energy (kcal·mol-1)	-19603.5	-19325.1	-18788.9	-18404.1	-17865.5	-17481.5
Max-Min (kcal·mol-1)			2122			
Density (g·cm-3)	1.831	1.832	1.824	1.799	1.796	1.776
Van der Waals force energy (kcal·mol-1)	-462.1	-457.5	-447.9	-390.6	-414.1	-362.2

As can be seen from Table 1 and Figure 2, with the decrease in temperature, the energy of CL-20/DNDA7 cocrystal decreases obviously. The total energy decreases from -18454.2 kcal·mol-1 to -20734.4 kcal·mol-1 and the energy decreases by 19.0 kcal·mol-1 for every 1K decrease. The energy is linear with the decrease in temperature. The CL-20/DNDA5 cocrystal energy decreases by 17.7 kcal·mol-1 for every 1K decrease and is slower than that of CL-20/DNDA7 cocrystal. The density of CL-20/DNDA7 and CL-20/DNDA5 super crystals varies from 1.755-1.847 g·cm-3 and 1.776-1.832 g·cm-3, CL-20/DNDA5 is slightly larger than CL-20/DNDA7, and the van der Waals force energy is slightly smaller. In terms of structure, DNDA7 has two more carbon chains than DNDA5, which provides a greater dispersion force than DNDA5. At the same time, more hydrogen atoms participate in the hydrogen bonds of the co-crystal system, which reduces the energy of the system. At the same time, more hydrogen atoms participate in the hydrogen bonds of the co-crystal system, which reduces the energy of the system. However, after the same carbon chains increase, the steric hindrance of the co-crystal becomes larger, and the density of the system decreases. Therefore, when preparing the cocrystal formation of CL-20 and linear ammonium nitrate explosive, the energy release characteristics and the difficulty of preparation should be considered.

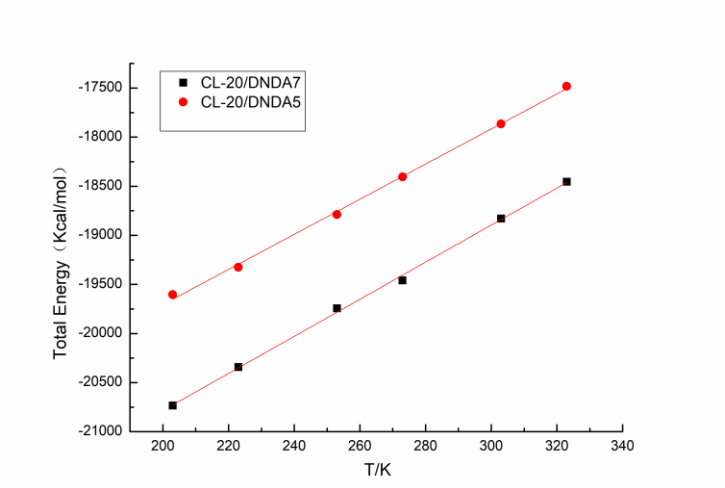

Figure 2. Variation of energy with temperature for three pressures in CL-20/DNDA7, CL-20/DNDA5 cells

3.2 Radial distribution function analysis

3.2.1 Analysis of O···H RDF

The O···H RDF was analyzed for the dynamics simulation results of CL-20/DNDA7 and CL-20/DNDA5 cocrystals. (Including CL-20 supplying the O atom and the ligand supplying the H atom and CL-20 supplying the O atom and the ligand supplying the H atom to form the hydrogen bond.) The O···H RDF of CL-20/DNDA7 and CL-20/DNDA5 cocrystals at different temperatures are shown in Figure 3 and Figure 4. The peak data are shown in Table 3.

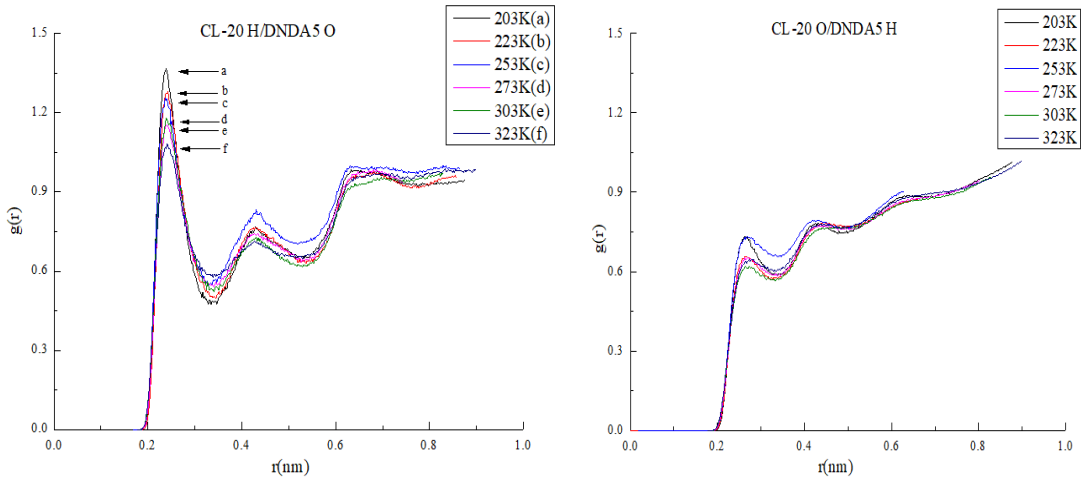

Figure 3. The O···H g(r) chart of CL-20 /DNDA7 at different temperatures

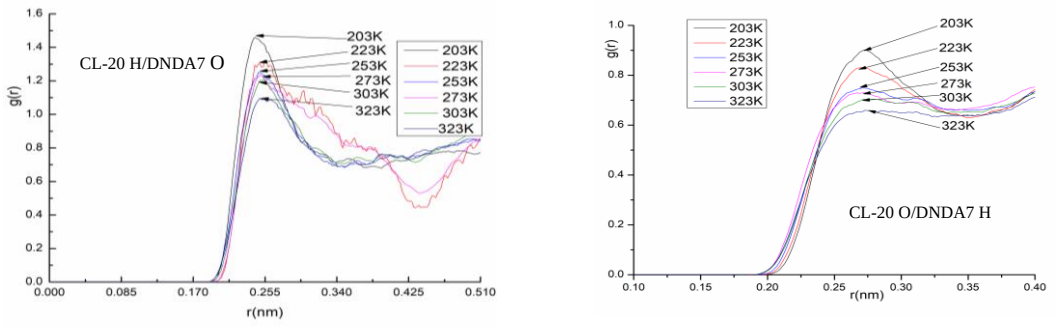

Figure 4. The O···H g(r) chart of CL-20 /DNDA5 at different temperatures

Table3 The O···H g(r) values of CL-20 /DNDA7 and CL-20 /DNDA5 at different temperatures

CL-20 H/DNDA7 O			CL-20 O/DNDA7 H		CL-20 H/DNDA5 O		CL-20 O/DNDA5 H	
T(K)	r(nm)	g(r)	r(nm)	g(r)	r(nm)	g(r)	r(nm)	g(r)
203	0.25	1.46	0.27	0.9	0.24	1.37	0.26	0.74
223	0.25	1.30	0.27	0.83	0.24	1.28	0.26	1.00
253	0.25	1.25	0.27	0.74	0.24	1.25	0.26	0.94
273	0.25	1.23	0.27	0.75	0.24	1.16	0.26	0.94
303	0.25	1.20	0.27	0.73	0.24	1.18	0.26	0.90
323	0.25	1.09	0.27	0.66	0.24	1.08	0.26	0.89

- As shown in Figure 3, Figure 4, and Table 3, the peak of the hydrogen bond between the H atom of CL-20 and the O atom of DNDA7 in the CL-20/DNDA7 cocrystal appears at 0.25 nm. As the temperature decreases (203K-323K), the g(r) value and the corresponding peak area become larger, i.e., the low temperature increases the hydrogen bond interaction. Especially when the temperature is 203K, the value of g (r) increases most obviously. This rule is consistent with the molecular dynamics simulation results of CL-20/DNDA5 cocrystal. The peak of the hydrogen bond between the O atom of CL-20 and the H atom of DNDA7 in the CL-20/DNDA7 cocrystal appears at 0.27 nm., and its bond length is larger than that formed when the H atom of CL-20 is provided, and the g(r) value is smaller. Therefore, the main driving force of the cocrystal formation between CL-20 and the linear ligand originates from the

hydrogen bond formed by CL-20 providing the H atom, and the linear ligand providing the O atom.

3.2.2 RDF analysis between CL-20 atoms

The RDF of the N-N bond of CL-20 in the cell of the CL-20/DNDA7 cocrystal was analyzed. The RDF curves of the N-N bond at different temperatures were shown in Figure 5. The N-N g(r) peak values of CL-20 in CL-20/DNDA7, CL-20/DNDA5 cocrystal and ε-CL-20 crystal are shown in Table 4.

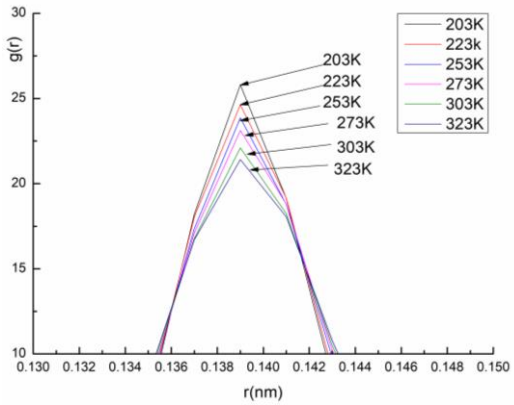

Figure 5. The N-N g(r) chart of CL-20/DNDA7 cocrystal at different temperatures

Table 4 The N-N g(r) peak values of ε--CL-20 and two cocrystals

Temperature/K	ε-CL-20 crystal	CL-20/DNDA7	CL-20/DNDA5
203	19.1	25.8	24.9
223	18.8	24.6	23.7
253	17.7	23.9	22.9
273	17.2	23.1	22.0
303	15.9	22.1	21.1
323	15.1	21.4	20.62

- According to Figure 5 and Table 4, when the temperature is 203K, the g(r) value of the N-N bond of CL-20 in CL-20/DNDA7 cocrystal is 25.8. The g(r) value of the N-N bond of CL-20 in the DNDA7 cocrystal cell is 25.8. With the increase in temperature, the value of g(r) decreases, the N-N bond of CL-20 is more easily decomposed, and the sensitivity increases; CL-20/DNDA5 and ε-CL-20 crystals have the same change. The g(r) value of ε-CL-20 crystal at 203K is 19.1, and that of CL-20/DNDA5 cocrystal is 24.9. The g(r) value of CL-20 is smaller than that of the two kinds of cocrystal, Therefore, the N-N bond strength of CL-20 was enhanced and the sensitivity was decreased by the cocrystal. Compared with the two cocrystals, the g(r) value of the CL-20/DNDA7 is always greater than that of CL-20/DNDA5 at the same temperature, and the N-N bond strength is slightly stronger, and its sensitivity is slightly lower. It can be speculated that with the increase of the carbon chain, the linear ligand is conducive to the low sensitivity of CL-20.

RDF analysis of N···O atoms of CL-20 in CL-20/DNDA7, CL-20/DNDA5 cocrystal, and

ε-CL-20 cell was carried out. The peak of g(r) values of N···O atoms at different temperatures are shown in Table 5.

Table 5. The N···O g(r) values of ε-CL-20 crystal and CL-20/DNDA7, CL-20/DNDA5 cocrystal

Temperature/K	ε-CL-20 crystal	CL-20/DNDA7	CL-20/DNDA5
203	36.3	49.3	48.1
223	35.4	47.5	46.9
253	33.3	45.5	44.5
273	32.2	44.7	42.9
303	31.2	42.8	41.2
323	30.0	41.5	40.2

As can be seen from Table 5, when the temperature is 203K, the g(r) value between N···O atoms of CL-20 in the CL-20/DNDA7 cocrystal is 49.3, and that of CL-20/DNDA5 cocrystal is 48.1 at the same temperature. According to the g(r) value of two kinds of cocrystal, The CL-20 nitro group in the CL-20/DNDA7 cocrystal is more stable than that in CL-20/DNDA5. With the decrease in temperature, the g(r) value of the three crystals increases, which means that cooling is conducive to reducing the probability of N-O bond decomposition.

3.3 Comparison of CL-20 with linear ligand cocrystal and CL-20/HMX cocrystal

3.3.1 Comparative analysis of bond lengths of initiating bonds

The maximum initiation bond length determines the beginning of the decomposition reaction, so the initiation bond length is an important parameter to evaluate the sensitivity of energetic materials. According to the results of g(r) values, the initiation bond of CL-20 and CL-20 cocrystal energetic materials is an N-N bond, so the sensitivity of energetic materials is compared by comparing the maximum bond length. Table 6 shows the maximum initiating bond lengths of CL-20 in the four crystals of ε-CL-20, CL-20/DNDA5, CL-20/DNDA7, and CL-20/HMX.

Table 6. The N-N bond maximum initiation bond length

crystals	ε-CL-20	CL-20/DNDA5	CL-20/DNDA7	CL-20/HMX
maximum initiation bond length（Å）	1.470	1.398	1.397	1.494

As can be seen from Table 6, the maximum initiating bond length of the ε-CL-20 is 1.470Å. The CL-20/DNDA5, CL -20/DNDA7, and CL -20/HMX cocrystals are 1.398 Å, 1.397 Å, and 1.494 Å, respectively. The maximum initiation bond lengths of the CL-20/DNDA5, and CL -20/DNDA7 cocrystals are both smaller than those of CL-20 and CL-20/HMX. Therefore, the cocrystal preparation of this type of energetic material with CL-20 is beneficial to reduce its sensitivity.

3.3.2 Comparison of Hirshfeld surface analysis

The 2D fingerprints of ε-CL-20, CL-20/DNDA5, CL -20/DNDA7, and CL -20/HMX cells are shown in Figure 6(a)-(d), and the O···H contact contributions to the Hirshfeld surface area in the *ϵ*-CL-20 crystal and cocrystals are shown in Table 7.

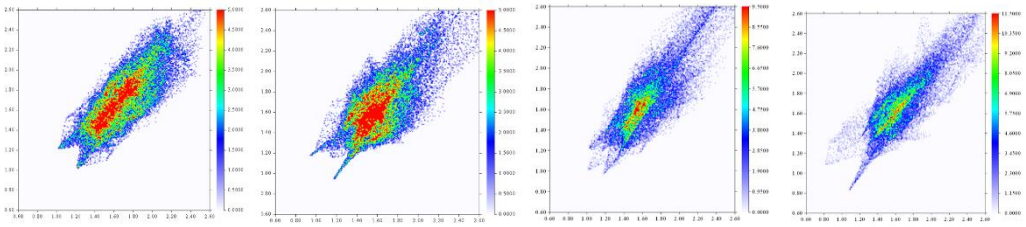

(a) (b) (c) (d)

Figure 6. The 2D fingerprints of CL-20(a), CL-20/DNDA5(b), CL-20/DNDA7(c), CL-20HMX(d)

Table 7. The Hirschfeld surface analysis contact contribution of the four structures

Contact type	CL-20/HMX (%)	CL-20/DNDA5 (%)	CL-20/DNDA7 (%)	ε-CL-20 crystals (%)
O ··· O	36.66	32.58	33.54	37.00
O ··· H	35.65	39.69	41.75	35.79
N ··· O	12.55	11.71	9.52	13.36
C ··· O	0	0	0	0
N ··· H	1.45	1.41	2.05	0.11
N ··· N	0	0	0	0.26
H ··· H	4.95	3.43	2.84	2.70

- As can be seen in Figure 6, The lower sharp peak represents the H···O atom interaction in the cell. In Figure 6 (d), the interaction peak of H···O atoms has obvious asymmetry and the O··· ·H interaction force of the central molecule CL-20 as hydrogen bond acceptor is significantly stronger than that of H··· ·O interaction force as hydrogen bond donor. Compared with CL-20/DNDA5 and CL-20/DNDA7 cocrystals, CL-20 is weaker as a hydrogen bond donor in CL-20/HMX cells.

As can be seen from Table 7, the O···H contact contributions of CL-20/HMX, CL-20/DNDA5, CL-20/DNDA7, and ε-CL-20 accounted for 35.65%, 39.69%, 41.75%, and 35.79%. The percentages of CL-20/HMX and ε-CL-20 are similar and significantly smaller than the other two cocrystals. So in terms of hydrogen bond interaction, the two linear nitroamine explosives have more advantages when combined with CL-20. From the perspective of structure, DNDA5 and DNDA7 have more hydrogen atoms. Although the main driving force of cocrystal formation depends on the hydrogen bond formed between the oxygen atoms provided by linear ligands and the hydrogen atoms on CL-20, in turn, CL-20 provides the nitro group, and the linear nitroamine explosive provides the hydrogen bond formed by the hydrogen atom, which plays an important auxiliary role. HMX is an eight-member ring structure, with 4 nitro groups on it and 8 hydrogen atoms on the ring. As the C-N bond on the eight-member ring structure is difficult to rotate and twist, hydrogen atoms connected with carbon atoms are

difficult to contact with oxygen atoms on CL-20, that is, it is difficult to form hydrogen bonds, and the auxiliary effect on CL-20/HMX eutectic is very weak, as can be seen from the finger diagram in Figure 6 (d). However, the straight-chain structure of linear ammonium nitrate explosive has a much higher degree of bending and folding than that of ring HMX, and it is more likely to contact oxygen atoms on CL-20, which makes the structure reach a stable state. Meanwhile, the structural steric hindrance of HMX is greater than that of these two linear nitroamine explosives, which also increases the difficulty of cocrystal formation.

3.3.3 Comparison analysis of growth simulation shape

The MS software of the Growth morphology module was used, the method of forcite is selected, the forcefield was selected as Compass, and Charges are selected as Forcefield assigned. The growth simulation of CL-20/DNDA5, CL-20/DNDA7, and CL-20/HMX cocrystal cells was carried out, and the results are shown in Figure 7(a)-(c). Figure 8(a) and (b) show the SEM images of CL-20/DNDA5 and CL-20/HMX cocrystal, respectively.

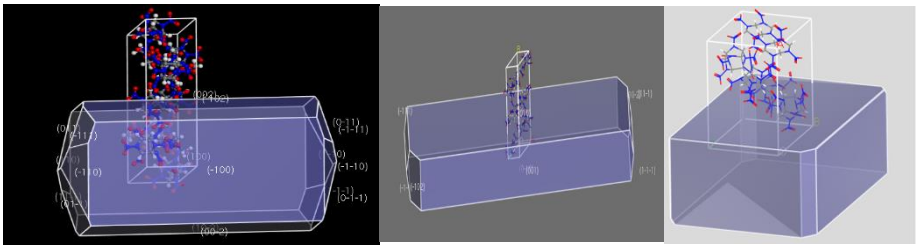

（a） （b） （c）

Figure 7. Growth simulation results for CL-20/DNDA5 (a), CL-20/DNDA7 (b) and CL-20/HMX (c) cocrystal

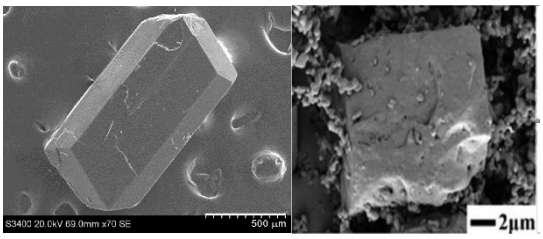

Figure 8. The SEM images of CL-20/DNDA5 (left) [36] CL-20/HMX [37] (right)

As can be seen from Figure 7, the morphology of the cocrystals a and b formed by the two linear ligands with CL-20 has no obvious tip, while c is the CL-20/HMX cocrystal, whose shape tends to be tetrahedron, and the edges and corners of the two oblique pairs have a small section. Figure 8 shows the SEM images of CL-20/DNDA5 and CL-20/HMX cocrystals prepared by Sun [33] and Zhang[22], respectively. The simulation results are in good agreement with the experimental results. In terms of shape, CL-20/HMX has very obvious edges and corners, which are easy to generate hot spots in the case of impact or friction, that is, the shape of this crystal structure has obvious disadvantages in terms of sensitivity.

4. Conclusion

(1) The energy of CL-20/DNDA7 cocrystal supercell decreases linearly with the decrease in temperature, and the density increases with the decrease in temperature.

(2) The decrease of temperature is beneficial to the increase of cocrystal hydrogen bond strength, that is, the decrease of temperature is beneficial to the preparation of cocrystal, especially when the temperature is 203K, the hydrogen bond interaction increases significantly.

(3) The maximum initiating bond length of CL-20 cocrystal with both linear nitramine explosives is smaller than that of CL-20 and CL-20/HMX cocrystal. That is, the cocrystal sensitivity of such energetic materials is smaller than that of CL-20 and CL-20/HMX. From the crystal growth surface, the two linear ligand cocrystals have a more rounded shape. The CL-20/DNDA5 and CL-20/DNDA7 cocrystals have a significant advantage over CL-20/HMX in terms of shape.

(4) Compared with CL-20/DNDA5 and CL-20/DNDA7, CL-20 is weaker as a hydrogen bond donor in CL-20/HMX cocrystals. CL-20 is more likely to form hydrogen bonds with linear nitroamine explosives.

Acknowledgments

The authors thank Accelrys for its Materials Studio software, T. Lu for Multiwfn software, and Theoretical and Computational Biophysics(TCB) Group for its VMD software during the preparation of the paper.

Conflicts of Interest

The authors declare no conflict of interest.

Data Availability Statement

The data that support the findings of this study are available from the corresponding author upon reasonable request.

Funding: This research was funded by the Education Department of Liaoning Province, grant number LG2019016.

References

1. Sonia T, Patrick B, Guy A, et al. Potential Use of CL-20 in TNT/ETPE-Based Melt Cast Formulations[J]. Propellants, Explosives, Pyrotechnics, 2008, 33(2): 103-108.
2. Ghosh M, Sikder A K, Banerjee S, et al. Preparation of reduced sensitivity co-crystals of cyclic nitramines using spray flash evaporation[J]. Defense Technology, 2020, 16(1): 188-200.
3. Cheng P. Y. Preparation and Theoretical Investigation of Aromatic Compound-Based Cocrystal Explosives[D]. Nan Jing University of Science and Technology, Nan Jing, 2016.
4. Zhang L. Y, Yuan J. M, Liu Y. C, et al. Molecular Dynamics Simulation of CL-20/TNT/DNB Ternary Cocrystal [J]. Science Technology and Engineering, 2018, 18(09): 223-228.
5. Liu H, Yang Z, He Y. H. Reactive Flow Propagation in CL-20/TNT Co-crystal Explosive Induced by Local High-Temperature Zones: ReaxFF Molecular Dynamics Simulations [J]. Chinese Journal of Energetic Materials, 2017, 25(07): 557-563.
6. Fu Y. Z, Kang Z. P, et al. Effect of Cocrystallizing and Mixing on Sensitivity and Thermal Decomposition Mechanisms of CL-20/DNB via MD Simulation [J]. Chinese Journal of Energetic Materials, 2017, 25(02): 94-99.
7. Hang G Y, Yu W L, Wang T, et al. Theoretical investigation of the structures and properties of CL-20/DNB cocrystal and associated PBXs by molecular dynamics simulation[J]. Journal of molecular modeling, 2018, 24(4): 97.
8. Hang G Y, Yu W L, Wang T, et al. Comparative studies on structures, mechanical properties, sensitivity, stabilities and detonation performance of CL-20/TNT cocrystal and composite explosives by molecular dynamics simulation[J]. Journal of molecular modeling, 2017, 23(10): 281.
9. Tao J, Wang Y. F, et al. Molecular Dynamics Simulation of CL-20/HMX Cocrystal and Blends [J]. Chinese Journal of Energetic Materials, 2016,24(04): 324-330.
10. Zhu Y T, Lu Y W, Gao B, et al. Synthesis, Characterization, and Sensitivity of a CL-20/DNP Spherical Composite for Security[J]. Materials (Basel, Switzerland), 2018, 11(7): 1-9.
11. Bolton O, Simae L R, Pagoria P F, et al. High Power Explosive with Good Sensitivity: A 2:1 Cocrystal of CL-20: HMX[J]. Crystal Growth & Design, 2012, 12(9): 4311-4314.
12. Ghosh M, Sikder A K, Banerjee S, et al. Studies on CL-20/HMX (2:1) Cocrystal: A New Preparation Method, Structural and Thermo kinetic Analysis[J]. Crystal Growth & Design, 2018, 18(7): 3781-3793.

13. Sun S H, Zhang H B, Liu Y, et al. Transitions from Separately Crystallized CL-20 and HMX to CL-20/HMX Cocrystal Based on Solvent Media[J]. Crystal Growth Design, 2018, 18(01): 77-84.
14. Zhang S J, Zhang J P, Kou K C, et al. Standard enthalpy of formation, thermal behavior, and specific heat capacity of 2HNIW·HMX Co-crystals[J]. Journal of Chemical & Engineering Data, 2019, 64(01): 42-50.
15. Dirk H, Peter G, Thomas H, et al. Investigation Of Crystal-lisation Conditions to Produce CL-20 /HMX Cocrystal for Polymer-bonded Explosives[J]. Propellants Explosives Pyrotechnics,2019,44(06):668-678.
16. Gosh M, Sikder A K, Banerjee S, et al. Studies on CL-20/HMX (2:1) Cocrystal: A New Preparation Method and Structural and Thermokinetic Analysis[J]. Crystal Growth Design, 2018, 18(07): 3781-3793.
17. Tan Y. W. Study on Preparation, Characterization, and Properties of CL-20/nitromidazole cocrystal[D]. North University of China,Tai Yuan, 2020.
18. Zhang S H, Zhao H L. Preparation and Characterization of LLM-105 Cocrystal Explosives[J]. Advanced Materials Research, 2014, 3051(1800): 251-255.
19. Xu H, Duan X, Li H, et al. A novel high-energetic and good-sensitive cocrystal composed of CL-20 and TATB by a rapid solvent/non-solvent method[J]. RSC Advances, 2015, 5(116): 95764-95770.
20. Yuan S, Gou B. W, Guo S. F, et al. Preparation, Characterization and Properties of A New CL-20/TKX-50 Cocrystal Explosive [J]. Chinese Journal of Explosives and Propellants, 2020, 43(02): 167-172+179.
21. Zhao S. S, Song X. L, Wang Y. Characterization of nano-CL-20/HMX cocrystal prepared by mechanical milling method [J]. Journal of Solid Rocket Technology, 2018,41(04): 479-482.
22. Song C. K, An C. W, Li H. Q. Preparation and Performance of Micro/nano CL-20/HMX Energetic Cocrystal Materials [J]. Initiators and Pyrotechnics, 2018(01): 36-40.
23. Wu X W, Liu Z H, Zhu W H. External electric field induced conformational changes as a buffer to increase the stability of CL-20/HMX cocrystal and its pure components[J]. Materials Today Communications, 2021, 26(3): 101696.
24. Liu Q, Xiao J J, Zhang J, et al. Molecular Dynamics Simulation CL-20/TNT Cocrystal Explosive[J]. Chemical Journal of Chinese Universities-Chinese, 37(3): 559-566.

25. Aldoshin S M, Aliev Z G, Goncharov T K, et al. Crystal structure of cocrystals 2, 4, 6, 8, 10, 12-hexanitro-2, 4, 6, 8, 10, 12-hexaazatetracyclo [5.5. 0.0 5.9. 0 3.11] dodecane with 7 Htris-1, 2, 5-oxadiazolo (3, 4-b: 3′, 4′-d: 3 ″, 4 ″-f) azepine[J]. Journal of Structural Chemistry, 2014, 55(2): 327-331.
26. Zhou J H, Shi L W, Zhang C Y, et al. Theoretical analysis of the formation driving force and decreased sensitivity for CL-20 cocrystals[J]. Journal of Molecular Structure, 2016, 1116:1-3.
27. Zhu S, Ji J C, Zhu W H. Intermolecular interactions, vibrational spectra, and detonation performance of CL-20/TNT cocrystal[J]. Journal of the Chinese Chemical Society, 2020, 67(10): 1-5.
28. Wang S. T, Hao Y. P, Ba S. H, et al. Theoretical Calculation into the Structures and MD Simulation of CL-20/DNDA5 Cocrystal[J]. Crystal Research and Technology, 2021, 56(11).
29. Tao, J, Wang X. F, Zhao S. X, et al. Molecular Dynamics Simulation of CL-20/HMX Cocrystal and Blends [J]. Chinese Journal of Explosives and Propellants, 2016, 24(04): 324-330.
30. Wang N, Su J, Guan H. B, et al. Simulation on Mechanic-thermal-chemical Response of CL-20/HMX Cocrystal under Shock Loading [J]. Chinese Journal of Explosives and Propellants, 2021, 29(04): 315-324.
31. Liu, H, Li Y, Ma Z. L, et al. Study on the Initial Decomposition Mechanism of Energetic Co-Crystal 2, 4, 6, 8, 10, 12-Hexanitro-2, 4, 6, 8, 10, 12-Hexaazaiso-Wurtzitane (CL-20)/1, 3, 5, 7-Tetranitro-1, 3, 5, 7-Tetrazacy-Clooctane (HMX) under a Steady Shock Wave[J]. Acta Physico-Chimica Sinica, 2019, 35(08): 858-867.
32. Sun T. Molecular Dynamics Simulation Study on the Structure and Properties of CL-20 Cocrystal and their Composite Material [D]. Nan Jing University of Science and Technology, Nan Jing, 2015.
33. Li L, Yin T, Wu B, et al. Preparation of CL-20/HMX Co-crystal by Microchannel Crystallization Based on Solvent/non-solvent Method [J]. Chinese Journal of Explosives and Propellants, 2021, 29(01): 62-69.
34. Pei B. L, Peng S, Cao R, et al. Study on the Influence of Feeding Molar Ratio on CL-20/HMX Co-crystal [J]. Initiators and Pyrotechnics, 2020(02): 48-52.
35. He Q. Q, Liu Y. C, Yan L. W, et al. Preparation of High Purity CL-20/HMX Cocrystal Explosive by Suspension Method[J]. Chinese Journal of Explosives and Propellants, 2018, 41(01): 82-85.

36. Genceli F E, Gartner R, Witkamp G J. Eutectic freeze crystallization of a 2nd generation cool-led disk column crystallizer for MgSO4·H2O system[J]. Cryst Growth, 2005, 275(1/2): 1369-1372.
37. Zhang M, Tan Y, Zhao X, et al. Seeking a novel energetic co-crystal strategy through the interfacial self-assembly of CL-20 and HMX nanocrystals[J]. CrystEngComm, 22(1): 61-67.